图书在版编目（CIP）数据

第二届亚洲材料电磁过程学术研讨会论文集 ／赫冀成主编 .— 沈阳 ：东北大学出版社，2005.9
ISBN 7-81102-186-2

Ⅰ. 第… Ⅱ. 赫… Ⅲ. ①材料电磁过程 ②学术研讨会论文集—亚洲 Ⅳ. Q4

中国版本图书馆 CIP 数据核字（2005）第 093423 号

出 版 者：东北大学出版社
地址：沈阳市和平区文化路 3 号巷 11 号
邮编：110004
电话：024—83687331（市场部） 83680267（社务室）
传真：024—83680180（市场部） 83680265（社务室）
E-mail：neuph @ neupress.com
http：//www.neupress.com
印 刷 者：沈阳市政二公司印刷厂
发 行 者：东北大学出版社
幅面尺寸：210mm×285mm
插 页：2
印 张：20.25
字 数：768 千字
出版时间：2005 年 9 月第 1 版
印刷时间：2005 年 9 月第 1 次印刷
责任编辑：文 韬 责任校对：米 戎
封面设计：唐敏智 责任出版：杨华宁

定 价：120.00 元

General Information

The 2nd Asian Workshop on Electromagnetic Processing of Materials (Asian－EPM2005) was held in the Meeting Hall of the Key Laboratory of EPM (Ministry of Education). Northeastern University, Shenyang, China, during 23rd to 25th May, 2005.

In 2004, the 1st Asian Workshop on EPM was held in Tokyo, Japan, promoted mainly by the scientists from Japan, Korea and China. The success of this workshop made a great contribution to EPM, the internationally booming research field. Asian－EPM2005 will provide scientists and scholars in this area a forum on all aspects of EPM, foster the exchange of ideas, techniques, experiments and enhance the international collaborations.

This workshop will be sponsored by the Branch Committee of Electromagnetic Metallurgy & Materials Science with High Magnetic Fields (the Chinese Society for Metals), the Division of Materials, Science & Technology Committee (Ministry of Education, China) and Northeastern University (China) and financially supported by "K. C. WONG Education Foundation, Hong Kong" and "National Natural Science Foundation of China".

Scope of the Workshop

Asian－EPM2005 will focus on the latest developments in

(1) Fundamentals
(2) Magnetohydrodynamics and numerical simulation
(3) EPM flow control and stirring
(4) EPM and solidification microstructure
(5) EPM applied to continuous casting
(6) High magnetic filed applied to materials processing
(7) Induction heating and melting
(8) Measurement and equipment

The contributions are expected to be oriented but not limited to the recent results in EPM.

Organization Committee

Chairman	**Ji-Cheng He**	*Northeastern University, China*
Co-Chairmen	**Liang Zuo**	*Northeastern University, China*
	Jian-Zhong Cui	*Northeastern University, China*
Secretary-General	**En-Gang Wang**	*Northeastern University, China*
Members:		
	Fu-Xiao Yu	*Northeastern University, China*
	Jian Cui	*Baoshan Iron & Steel Co., LTD, China*
	Jing-Jie Guo	*Harbin Institute of Technology, China*
	Lin Liu	*Northwestern Polytechnology University, China*
	Ting-Ju Li	*Dalian University of Technology, China*

Wei Liu	*Tsinghua University, China*
Yuan-Sheng Yang	*Institute of Metal Research, CAS, China*
Zhong-Ming Ren	*Shanghai University, China*

International Advisory Committee

Gunter Gerbeth	*Forschungszentrum Rossendorf, Germany*
Heng-Zhi Fu	*Northwestern Polytechnology University, China*
Ho-Young Kim	*POSCO, Korea*
Joon Pyo Park	*Research Institute of Industrial Science & Technology, Korea*
S. Ranganathan	*Indian Institute of Science, India*
Shigeo Asai	*Nagoya University, Japan*
Shoji Taniguchi	*Tohoku University, Japan*
Takehiko Toh	*Nippon Steel Corporation, Japan*
Tie-Yong Zuo	*Beijing University of Technology, China*
Yasuo Kishimoto	*JFE Steel Corporation, Japan*
Yves Fautrelle	*Institut National Polytechnique de Grenoble, France*
Zhuang-Qi Hu	*Institute of Metal Research, CAS, China*

Contact Address

Professor **En-Gang WANG**

Key Laboratory of EPM (Ministry of Education), Northeastern University
Add: P. O. Box 314, Northeastern University
No. 3-11, Wenhua Road, Heping District, Shenyang, 110004, China
Tel: +86-24-83681739, 83681758
Fax: +86-24-83681758
Email: egwang@ mail. neu. edu. cn

Section 1

Invited Lecture

Recent EPM Activities in Nagoya University

Shigeo Asai
Nagoya University, Furo-cho, Chikusa, Nagoya, 464-8603, Japan

Abstract: EPM activities in Nagoya University in the last two years are classified in the application of Lorentz force and Magnetization force. The former is (1) development of a magnetic valve and (2) visual simulation of bubble behavior in a molten metal under a magnetic field. (3) in situ measurement of phase transformation, (4) crystal orientation of ceramics in a slip casting and sintering processes, and (5) composite crystal orientation in HAp and collargen are belong to the latter. Here (1), (3) and (4) are briefly described together with future prospect.

1. Introduction

In the last 2 years we have mainly involved into EPM relating to a high magnetic field. This activity has started 1990s by introducing a helium free super-conducting magnet, which was the second one in this type magnets produced by a Japanese company and now they say about 250 magnets in the type are running through Japan, mainly in academic field. At first we were excited by facing various new phenomena observed under a high magnetic field. Then our interest was led to functions which can be introduced only by use of a high magnetic field, such as crystal orientation and enhancement of a small current based on magnetization force and Lorentz force, respectively. Now most of phenomena accompanied by a high magnetic field, except a few examples, are able to be classified into the known functions and people pay more attention to the industrial application of a high magnetic field. In this paper the recent activities of EPM in Nagoya University are introduced. And the future prospect is discussed.

2. Application of high magnetic field in EPM

2.1 Classification of functions accompanied by high magnetic field

Owing to the development of super conducting technologies, by which a high magnetic field with rather large space is now available even in conventional scale laboratories, the technology relating to crystal orientation, structure alignment and spin chemistry has first been introduced in EPM. Table 1 indicates the classification of functions accompanied by a high magnetic field in EPM. The high magnetic field enables not only to enhance the various functions based on Lorentz force but also to induce several functions based on the magnetization force. The crystal orientation and the structure alignment in non-magnetic materials are typical examples introduced by use of the magnetization force. Four necessary conditions have to be satisfied for the crystal orientation under the imposition of a magnetic field. Firstly

Tel. 81-52-789-4646, Fax. 81-52-789-3247, e-mail: asai@numse.nagoya-u.ac.jp

a unit crystal cell of materials to be oriented should have a magnetic anisotropy. The second is that the magnetization energy provided by magnetic field should be larger than thermal energy to lead to thermal perturbation. The third condition is that the materials should exist in the weak constraint medium in which a particle composed by the materials can rotate by such a feeble magnetization force. The fourth is that each particle composed by a single crystal should be dispersed in the medium.

Table 1 Utilization of a high static magnetic field in EPM

- Lorentz Force
  - Strong brake effect in liquid metal flow
  - Enhancement of Lorentz force in small electric current
- Magnetization Force
  - Mass Transport —— Elimination of inclusions and surface defect
    $(\chi/\mu)(B\cdot\nabla)B$
  - Mass Rotation (Torque) MxB
    - Crystal orientation
      - vapor-deposition
      - electro-deposition
      - magnetic slip casting
      - organic molecular reaction
    - Structural alignment phase transformation
- Magnetization energy —— Crystal orientation accompanied by crystal growth
- Spin Chemistry —— Intermolecular cross-linking reaction

The possibility of mass transport and mass rotation due to the magnetization force was studied under several processes such as solidification[1-4], electro-deposition[5] vapor-deposition[6-8] and solid phase reaction[9]. Now people have recognized the application of a high magnetic field is surely useful and promising methods in EPM.

2.2 Magnetic valve of molten metal flow

A static magnetic field has a function to suppress a molten metal flow, which has already been applied on a single crystal production of silicon industry as a magnetic Czochralski method and a steel production as a magnetic brake in a continuous casting process. In these cases, the magnetic flux density is 0.5 T at most.

A molten metal flow in a duct channel under a magnetic field is called a Hartmann problem, where the braking effect is drastically increased by increasing a field intensity up to 5~10 T. In order to demonstrate the braking effect, the mean metal flows from a tank with metal height of 60mm were observed in a model experimental apparatus shown in Fig. 1. At 5 T, a channel metal flow was declined to about 7/1000 of the flow without magnetic field. This result suggests that the function of suppressing of a metal flow is useful and will be used in a metals industry in the near future accompanying with the further development of superconducting technologies.

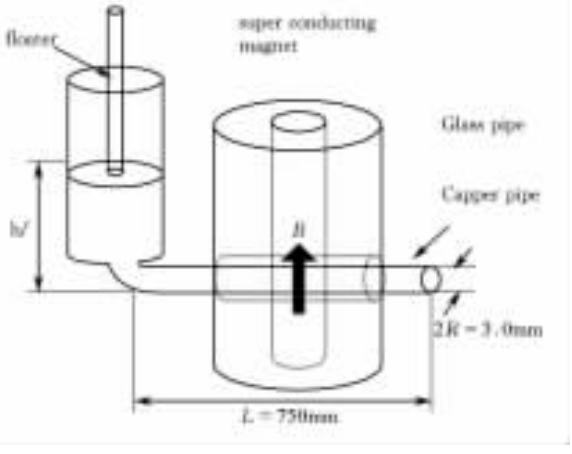

Fig. 1 Experimental apparatus

Furthermore, a magnetic dam is available by simultaneous imposition of a high magnetic field and an electric current. This is also a promising technology in metal processes such as galvanization, ejecting

of molten metal from a cold crucible and a side dam of a twin roll casting. Fig. 2 demonstrates that a stable holding of a molten metal is available under the conditions between the simultaneous imposition of 4 T and 0.91 A and 4T and 1.5A. Under the condition of 4T and 0.7A the front of a molten metal coming from a right hand side of an upwind side was almost held between electrodes but not be completed. That is, it passed through the portion of the electrodes after 15 seconds. The other hand under the condition of 4T and 1.74A the front was deeply depressed toward the upwind side, and at 4T and 2.1A an unstable switching behavior which repeats touching and detaching electrodes was observed.

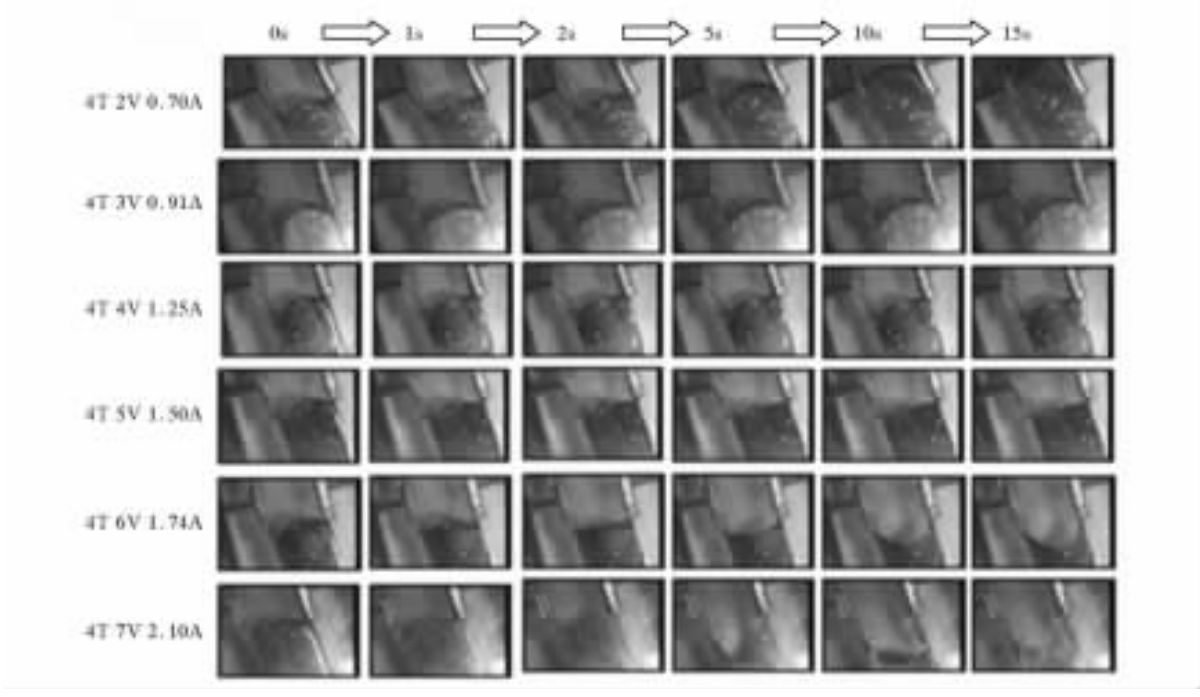

Fig. 2 A molten metal behavior between electrodes

3. Qualitative evaluation of phase transformation

3.1 Principle

A magnetic susceptibility of a mixture with two components is given by Eq (1).

$$\chi_m = f_1\chi_1 + f_2\chi_2 \tag{1}$$

where f_1 and f_2 are a fraction of the two components, respectively. In addition, Eq. (2) holds obviously.

$$f_1 + f_2 = 1 \tag{2}$$

Once the magnetic susceptibility χ_m is measured, the fractions of each component in the mixture can be derived from Eqs. (1) and (2).

$$f_l = \frac{\chi_m - \chi_2}{\chi_1 - \chi_2},\ f_2 = \frac{\chi_m - \chi_1}{\chi_2 - \chi_1} \tag{3}$$

Here, the magnetic susceptibility can be obtained by the use of Gouy method [10, 11] which is based on the

measurement of a magnetization force F_z. as Eq. (4).

$$\chi_m = \frac{2L\mu_0}{m_s (B_L^2 - B_0^2)} F_z \tag{4}$$

where L and m_s are a length and a mass of the specimen, respectively. μ_0 is a magnetic permeability and B_L and B_0 are magnetic flux densities at the top and bottom of the specimen, respectively. And the magnetization force F_z can be obtained from the difference between the weights of a specimen measured under the imposition with and without magnetic field.

When we apply the principle to evaluate a phase fraction change during a phase transformation, we have to measure a temperature of the specimen together with the magnetization force since the magnetic susceptibility is a function of temperature to evaluate the values of χ_1 and χ_2. appearing in Eq. (3) beforehand.

3.2 Measuring solid fraction during solidification

We can figure the relationship between the magnetic susceptibility and temperature measured during the solidification of an alloy as shown in Fig. 3. It is found that the magnetic susceptibilities of solid and liquid phases can both be expressed as a linear function of the temperature around the melting point with a good approximation. That is, the magnetic susceptibilities in the single solid and liquid phases are given by Eqs. (5) and (6).

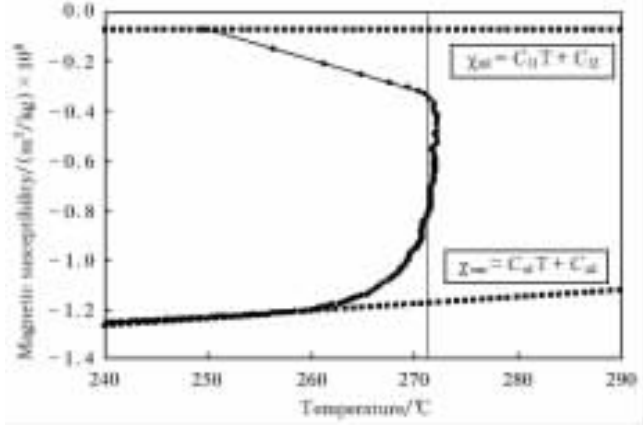

Fig. 3 Calculation of solid fraction

$$\chi_{ml} = C_{11} T + C_{12} \tag{5}$$

$$\chi_{ms} = C_{s1} T + C_{s2} \tag{6}$$

By substituting χ_{ml} and χ_{ms} evaluated from Eqs. (5) and (6) into Eq. (3), the relation between the solid fraction and temperature during solidifying of Zinc is obtained as Fig. 4. It is noticed that the solid phase of about 50mass% has precipitated at the moment when the recalescence finishes and the temperature comes back to the melting point.

3.3 Phase transformation from γ phase to α phase in carbon steel

Let us consider the phase transformation from γ to α in carbon steel taken place above the Curie point, where γ and α phases are paramagnetic. Eqs. (1), (2) and (3) are expressed as Eqs. (7), (8) and (9), respectively.

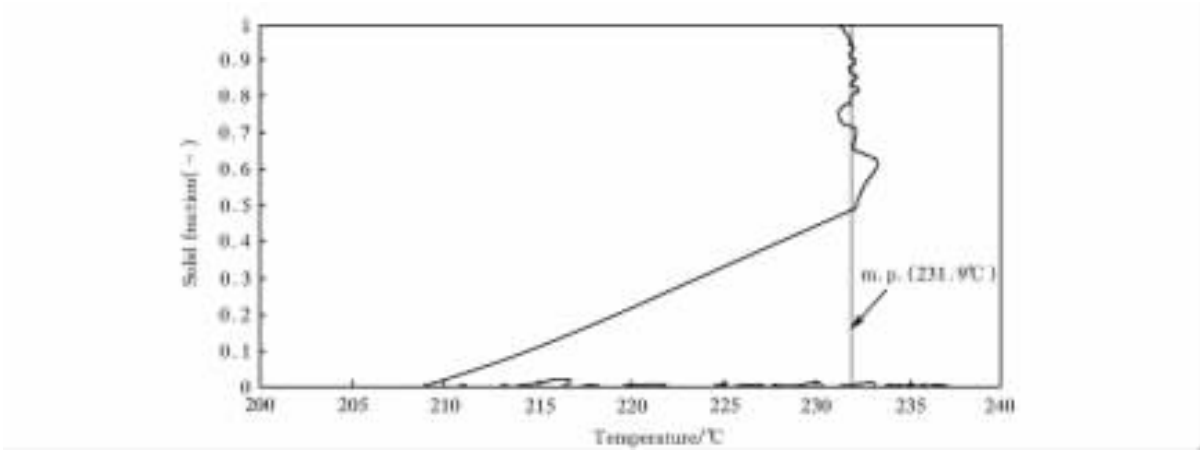

Fig. 4 The relation between temperature and solid fraction for Zinc (cooling)

$$\chi_m = f_\alpha + f_\gamma \tag{7}$$

$$I = f_\alpha \chi_\alpha + f_\gamma \chi_\gamma \tag{8}$$

$$f_\alpha = \frac{(\chi_m - \chi_\gamma)}{(\chi_\alpha - \chi_\gamma)} \tag{9}$$

When a specimen kept in γ phase is suddenly put into a temperature where the phase transformation from γ to α takes place, the transitional fraction of α phase is given by Eq. (9). At the equilibrium where the phase transformation γ to α has finished, the value of χ_m and α phase fraction f_α are obtained as the $\chi = \chi_e$, which is the observed value at the equilibrium and $f_\alpha = \frac{b}{a+b}$, which is obtained from a phase diagram as shown in Fig. 5. Then those are substituted into Eq. (9), χ_α is obtained by Eq. (10) and the value of χ_γ is given as the measured value of χ_m at $t = 0$.

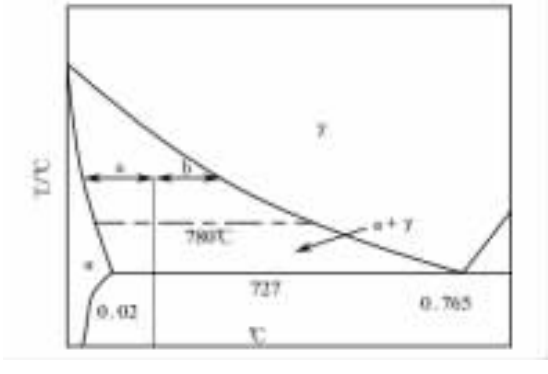

Fig. 5 Fe-C phase diagram

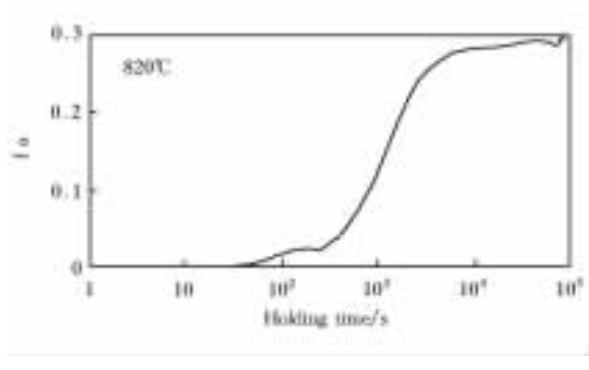

Fig. 6 Transitional phase fraction of α in γ − α phase transformation.

$$\chi_\alpha = \frac{a+b}{b}\chi_e - \frac{a}{b}\chi_e \tag{10}$$

A specimen with a size of 2mm × 2mm × 0.5mm and 0.2C% steel encapsulated in a glass tube was kept at 950℃ for 30 min. under a magnetic field of 5T and then the temperature was quickly changed to 820℃ and kept there to induce the γ-α phase transformation under the magnetic field. The transitional

phase fraction of f_α is shown in Fig. 6.

As the method developed here can be applied to in-situ measurement of various phase transformation in solid, liquid and gas phases, I hope it will provide the better and deeper understanding of phase transformations and reactions in the near future.

4. Crystal orientation in high magnetic field

4.1 Introduction

Recently, it has been found that the crystal orientation in materials can be controlled by imposition of the high magnetic field. This principle can be applied not only to magnetic materials but also to non-magnetic materials with asymmetric unit cells[12-22]. When materials are placed in a magnetic field, crystals exhibiting anisotropic magnetic susceptibility orient themselves to the direction of the maximum susceptibility parallel to the magnetic field direction.

In this chapter, the effect of a high magnetic field on the crystal orientation has been studied in two processes. In the first process using a slip casting operation, a crucible containing ceramic slurry was rotated under a high magnetic field to fabricate textured ceramics with one directional crystal orientation. In the second process, a green sample with some amount of oriented crystals which was initially introduced by the slip casting under a high magnetic field was sintered in a high magnetic field. In the sintering process, the effects of intensity of the magnetic field and the initially introduced amount of oriented crystals on the total crystal orientation in final products were studied.

4.2 Theory of crystal texture controlled by magnetic field theory

4.2.1 Magnetization energy

When a non-magnetic substance is magnetized in a magnetic field, the energy for magnetization of the substance is given by Eq. (11).

$$U = -\int_0^{B/\mu_0} M \mathrm{d}B_{in} \tag{11}$$

where M is the magnetization, B and B_{in} the imposed magnetic flux density and the magnetic flux density appeared in the substance, respectively, μ_0 the permeability in vacuum ($4\pi \times 10^{-7}$ [H/m]). The principle to control the crystal orientation using a magnetic field is that a magnetic torque rotates crystals to take the stable crystal orientation so as to decrease the magnetization energy.

Let us consider ceramics of the crystal structure with a magnetic anisotropy, that is, the magnetic susceptibility is different in each crystal direction. The value of the magnetization energy given by Eq. (12) that is derived from Eq. (11), determines the preferred crystal direction depending on the magnetic susceptibility of each crystal axis and the crystal shape.

$$U = -\frac{\chi}{2\mu_0 (1 + N\chi)^2} B^2 \tag{12}$$

where N is the demagnetization factor. Let χ_c and $\chi_{a,b}$ represent c-axis and a- or b-axis of a magnetic susceptibility, respectively. When, $\chi_c > \chi_{a,b}$, i.e. $U_c < U_{a,b}$, c-axis of crystals is the preferred axis in parallel to the direction of magnetic field. In contrast, when $\chi_c < \chi_{a,b}$, i.e. $U_c > U_{a,b}$, a-or b-axis of crystals is the preferred axis in parallel to the magnetic field, that is, c-axis of crystals aligns to all of

the directions in the plane perpendicular to the imposed magnetic field.

4.2.2 Classification of particle size

Regarding the crystal orientation using the magnetization force, we have to discuss effects of the magnetization force by classifying particle size. For a large particle, the gravity force must be taken into consideration, while the Brownian motion can be ignored. The terminal velocity due to the gravity force is given by Eq. (13).

$$v_T = \frac{2g(\rho_p - \rho_l) r^2}{9\eta_0} \tag{13}$$

Here, v_T is the terminal settling velocity of the particle, g the acceleration of gravity, r the radius of a particle, η_0 the viscosity coefficient of the medium, ρ_l and ρ_p the density of the medium and particle, respectively. For a spherical particle, the alignment time τ_m under a high magnetic field can be evaluated by Eq. (14).

$$\tau_m = \frac{6\eta_0\mu_0}{\Delta\chi B^2} \tag{14}$$

Here, μ_0 is the magnetic permeability of vacuum ($4\pi\times10^{-7}$ [H/m]), $\Delta\chi$ the difference between magnetic susceptibilities in crystal axes, B the imposed magnetic flux density. The crystal rotation due to the magnetization force must finish before the particle sediments to the bottom of a crucible. By considering falling length L, this condition can be expressed as:

$$\tau_m < \frac{L}{T} \tag{15}$$

By substituting Eqs. (13) and (14) into Eq. (15), the maximum radius of a particle which can be aligned by the magnetization force is given as Eq. (16).

$$r_{max} < \sqrt{\frac{3\Delta_\chi B^2 L}{4\mu_0 g(\rho_p - \rho_l)}} \tag{16}$$

For a small spherical particle suspended in a fluid, the displacement due to Brownian motion can be expressed as:

$$x(t) = \sqrt{\frac{2DkT}{\zeta}[t - \tau_R(1 - e^{-t/\tau_R})]} \tag{17}$$

where $\zeta = 6\pi\eta_0 r$ is the friction coefficient, and $\tau_R = \frac{m}{\zeta} = \frac{2\rho_p r^2}{9\eta_0}$ the relaxation time, which means the time constant for getting to an equilibrium state of system after a disturbance. Here, D is the numbers of dimensions of space, k Boltzmann constant (1.38×10^{-23}J/K), T the temperature, t time. Within the relaxation time of τ_R, if the average velocity of a particle caused by Brownian motion is lager than the terminal settling velocity caused by the gravity force, then the gravity force can be ignored. In addition, since only the direction of gravity is considered here, D equals to 1. Therefore, a following equation can be obtained.

$$\frac{x(\tau_R)}{\tau_R} > v_T \tag{18}$$

The critical radius of a particle, which is determined by Brownian and gravity motions, is derived from Eqs. (13), (17) and (18) as Eq. (19).

$$r_{Cri} = 7\sqrt{\frac{243kT\eta_0^2}{8\pi e g^2 \rho_p (\rho_p - \rho_l)^2}} \tag{19}$$

In other words, for the orientation of particles under a high magnetic field, we don't need to consider the gravity force when the radius r is smaller than r_{Cri}.

The minimum critical particle size is determined as follows; for the rotation of a particle, the rotational relaxation time in Brownian motion is given by Eq. (20).

$$\tau_B = \frac{3v\eta_0}{kT} \tag{20}$$

Here, v is the volume of the particle. It is known that Brownian motion is more active for smaller particle. In order to effectively align particles under a high magnetic field, the particle must be large enough to overcome Brownian motion. The orientation time must be shorter than the relaxation time for Brownian motion. This condition is expressed as Eq. (21).

$$\tau_m < \tau_B \tag{21}$$

From this equation, the minimum radius of a particle which can be aligned is determined as Eq. (22).

$$r_{\mathrm{m}} > 3\sqrt{\frac{3kT\mu_0}{2\pi\Delta\chi B^2}} \tag{22}$$

Equation (22) gives the critical minimum particle size necessary for orientation under a high magnetic field. According to the critical particle sizes mentioned above, the effective particle size for orientation under a high magnetic field is schematically shown in Fig. 7.

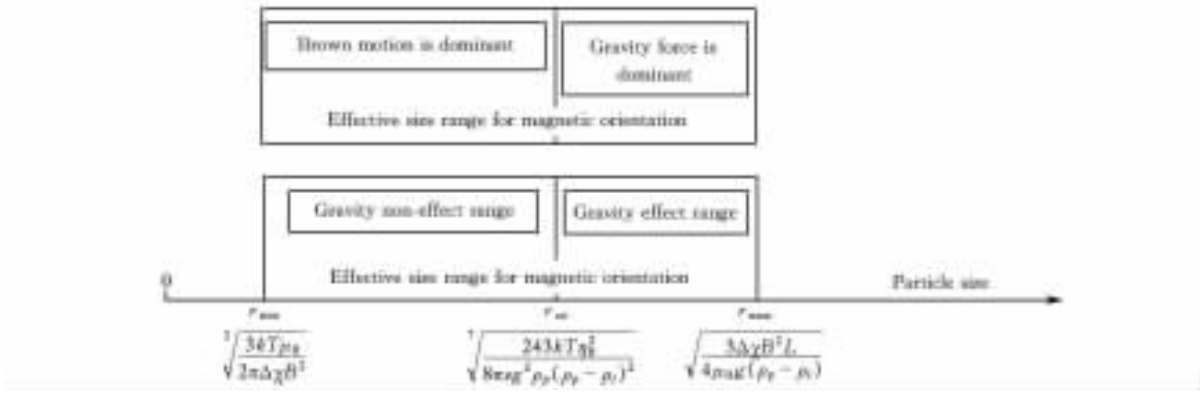

Fig. 7 Effective spherical particle size for orientation under a high magnetic field

When applying a high magnetic field, the range of effective particle size for orientation can further be classified into:

Case 1:
$$3\sqrt{\frac{3kT\mu_0}{2\pi\Delta\chi B^2}} < r < 7\sqrt{\frac{243kT\eta_0^2}{8\pi eg^2\rho_p(\rho_p-\rho_l)^2}};$$

In this case, Brownian motion is dominant and the gravity force can be ignored. In other words, for orientation of the particles sized in this range, we don't need to consider the gravity force, but only Brownian motion and magnetic field effect.

Case 2:
$$7\sqrt{\frac{243kT\eta_0^2}{8\pi eg^2\rho_p(\rho_p-\rho_l)^2}} < r < \sqrt{\frac{3\Delta_\chi B^2 L}{4\mu_0 g(\rho_g-\rho_l)}};$$

In this case, gravity force is dominant, while the Brownian motion can be ignored. That is to say, only gravity force and magnetic field take effects for particles in this size range.

4.3 Control of crystal orientation

4.3.1 Application of magnetic field in slip casting process

A novel process where a high magnetic field is imposed during slip casting was proposed to fabricate highly crystal-orientated ceramics[24, 25]. Here, another novel process is proposed, in which a specimen is rotated during the slip casting under a high magnetic field. Fig. 8 schematically shows functions of

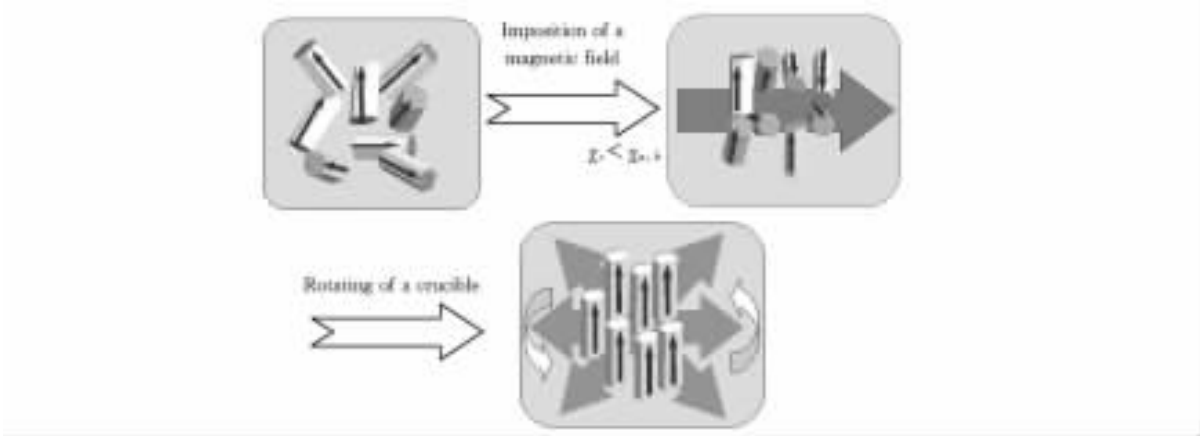

Fig. 8 Schematic views showing the functions of magnetic field and rotation of a crucible under a magnetic field

magnetic field and rotation of crucible. Regarding the substance whose magnetic susceptibility in a or b axis is higher than that in c-axis, $\chi_c < \chi_{a,b}$, one-directional crystal orientation can not be obtained in a slip casting under a high magnetic field, because the free choice of crystal orientation exists both in a and b axes. When the magnetic field is imposed on the suspension, the c-axis of particles can align to various directions in the plane that is perpendicular to the magnetic field direction. When a rotating magnetic field is imposed on a fixed specimen, c-axis of particles will be perpendicular to the plane in which the magnetic field is rotating. From the view point of the relative motion, the condition where the specimen is fixed and the magnetic field rotates is equivalent to the case where the specimen rotates in the fixed magnetic field. Fig. 9 shows the schematic view of the experimental apparatus with rotation of the specimen. In this configuration, it suggests that the c-axis of particles will align to the direction parallel to the gravity direction. The usefulness of the newly proposed process has been confirmed in fabrication of Si_3N_4 ceramics. In order to examine the effect of rotation, green samples were prepared by rotating under the magnetic field of 10T. Moreover, for the sake of comparison, another sample was also made without magnetic field. After drying, the green samples were embedded in powder bed of 60wt%Si_3N_4 + 40 wt% BN set in a graphite crucible and heated at the temperature of 1800℃ for 1.5hrs in N_2 atmosphere without a magnetic field. Fig. 10 shows the SEM micrograph of the polished surfaces of specimen. It also can be seen in Fig. 10. (a) and (b) that β-Si_3N_4 rod grains appear randomly distributed in the specimen which was prepared without exposure to the magnetic field. In the case of the specimens prepared with the rotation under magnetic field, a highly textured material was obtained as shown in Fig. 10 (c) and (d).

4.3.2 Crystal orientation of hydroxyapatite in a sintering process

4.3.2.1 Introduction

Hydroxyapatite (HAp) is the main component of bones and teeth of vertebrates. The crystals of

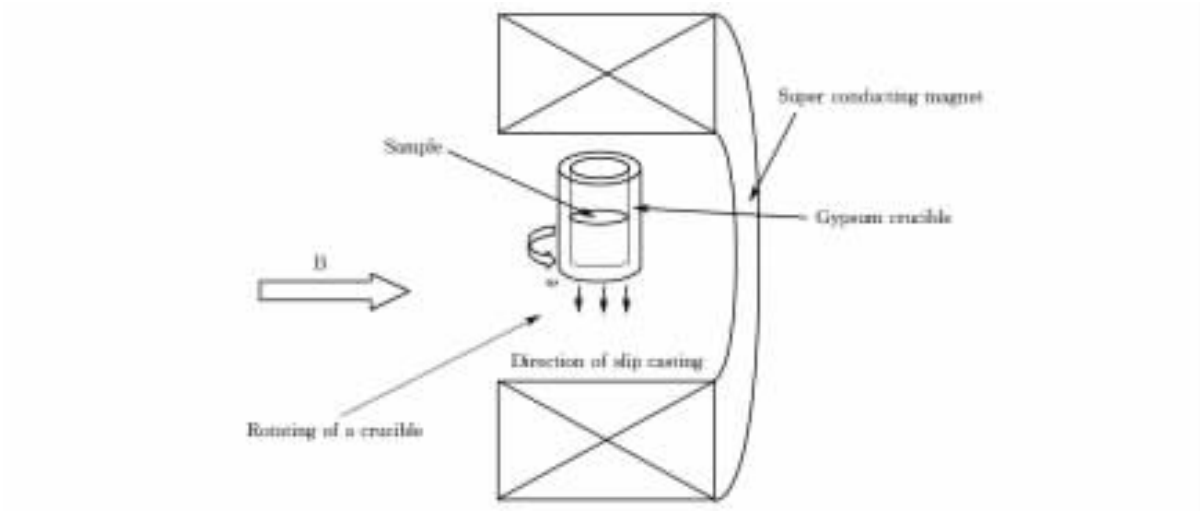

Fig. 9 Schematic view of experimental apparatus for rotation of a crucible under a magnetic field

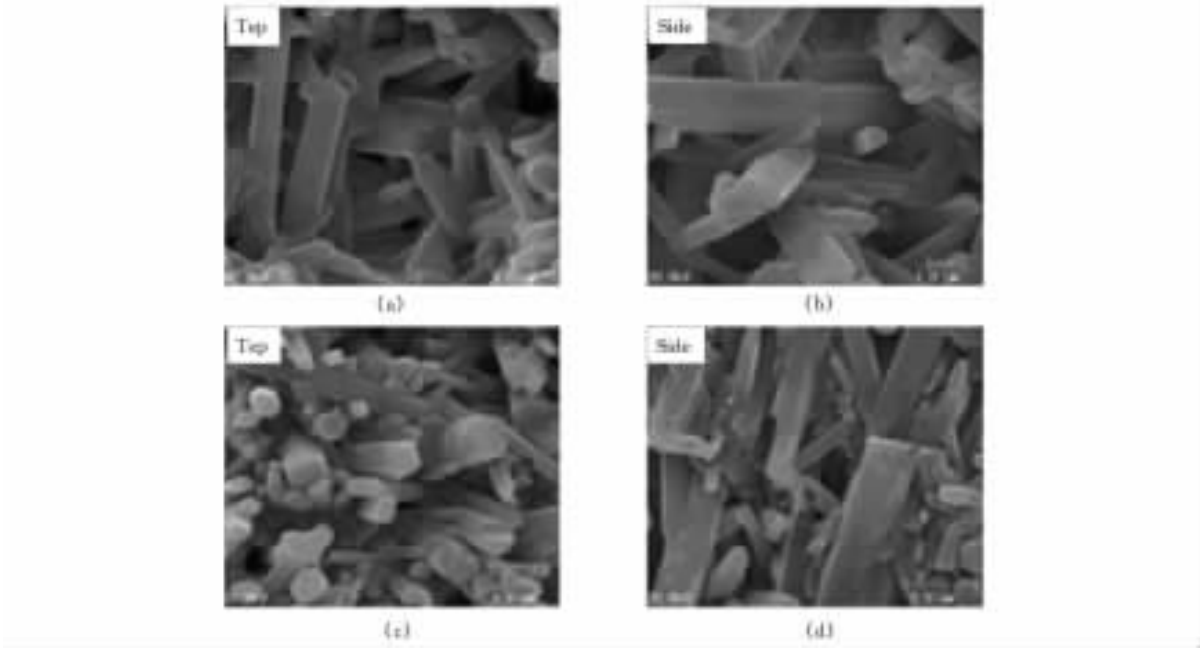

Fig. 10 SEM micrographs of specimens made of □-Si_3N_4 powder with □- Si_3N_4 seeds
(a), (b) without magnetic field, (c), (d) with magnetic field of 10T under rotation of crucible

HAp are highly oriented. HAp has been used as biomaterials with brilliant biocompatibility and bioactivity, which can be so improved by controlling over the crystal orientation as to bear resemblance to textures of bone or tooth. HAp is also useful as a protein adsorbent in a liquid chromatography. Hence the orientation control of HAp crystals is important for using not only as the biomaterials but also as protein absorbents.

Here, in the sintering process the effects of the intensity of a high magnetic field and the amount of the oriented crystals, which were initially introduced in a green sample by using slip casting, on the crystal orientation of HAp are studied. The experimental results have been simulated by a Potts model modi-

fied here.

4.3.3.2 Experiment and result

A green compact was formed by using the slip casting under a high magnetic field of 10T. That is, the magnetic field was imposed on the slurry in parallel with the direction of the slip casting and dried in air over 24 hrs without magnetic field. Then it was sintered at 1423K for 2 hrs with or without the magnetic field of 10T, which was imposed at the same direction as that in the slip casting. The sintered compact was examined by means of X-ray diffraction analysis, which was carried out on the surface perpendicular to the direction of the imposed magnetic field in the slip casting and sintering processes.

The relative facial angle [26] of the samples is shown in Fig. 11. The relative facial angle increases from 61.0 to 69.0 degrees, when the magnetic field was imposed during the slip casting. When no magnetic field was imposed during the slip casting, the magnetic field in the sintering process changed the relative facial angle from 61.2 to 64.9 degrees. This fact implies that the effect of the magnetic field in the sintering is detectable, but little. On the other hand, when the green samples were prepared using the slip casting under the magnetic field, the relative facial angle increased from 69.0 to 72.4 degrees by the sintering without the magnetic field, and increased from 69.0 to 83.1 degrees by the sintering with the magnetic field. These results indicate that HAp crystals were highly orientated by imposing the magnetic field on the sintering and slip casting processes.

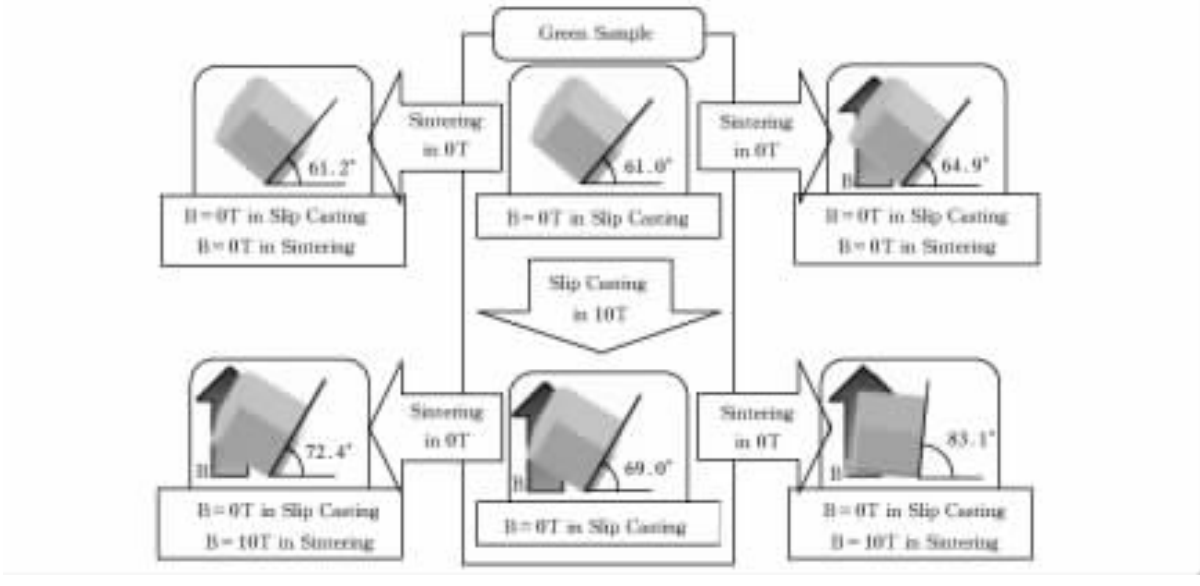

Fig. 11 Relative facial angles from c-plane of samples

4.3.3.3 Discussion

As the oriented crystals could not obtained in a green sample by using the slip casting without a magnetic field, the imposition of the magnetic field in the sintering process did not have a significant effect on the crystal orientation. However, the slip casting with the magnetic field introduces some amount of the oriented crystals in the green sample, which could preferentially agglomerate in the sintering process, because the interface energy of the oriented crystals contacting with same orientation each other is lower than that of non-oriented crystals. Thus, the oriented crystals agglomerate more quickly than the non-oriented crystals. Furthermore, Ostwald-Ripening mechanism works to enlarge the agglomerated

crystals with a larger diameter rather than the non-oriented crystals with a small diameter. That is, the double effects of the agglomeration and ripening mechanisms accelerate the crystal orientation in the sample that was treated by the imposition of a magnetic field in the slip casting and sintering processes.

Potts model [27] using a Monte Carlo method has been adopted to simulate the crystal growth in the sintering process with a magnetic field. In the simulation, the amount of the initial oriented crystals, which are labeled a zero indicating crystal orientation, was changed as 10%, 12%, 15%, 18% and 20%. The calculated results with different amount of the initial oriented crystals are shown in Fig. 12. In the case of taking no account of magnetic effect in the sintering process, the initial oriented crystals of 10% in the green sample do not contribute to provide any further crystal orientation with time. The effect of the crystal orientation appears when the amount of the initial oriented crystals is more than 12% even if the magnetization energy effect is not taken into account. On the other hand, in the case taking account of the magnetic field effect in the sintering, the crystal orientation is slightly enhanced even if the initial oriented crystals of 10% are introduced. If the initial oriented crystals are more than 12%, the crystal orientation is further enhanced in comparison with the case of taking no account of the magnetic field effect. The increasing rate of the crystals aligned to the preferred orientation for the imposed magnetic field is shown in Fig. 13. The magnetic effect on the crystal orientation is more largely enhanced with the increase in the initial oriented crystals, and reaches the maximum at 18%, and inversely turns down at 20% due to the insufficient amount of residual non-oriented crystals. The experimental results also indicated that the effect of magnetic field scarcely appeared when the initial oriented crystals were not introduced, but became prominent once the initial oriented crystals were introduced in the green samples. The evidence found in the experiment has been well reproduced by this Potts model simulation, which has taken account of effect of the crystal orientation due to magnetic crystal anisotropy. The knowledge obtained in the study could be applied to not only HAp but also various ceramic and metal crystals with magnetic anisotropy.

5. Future prospect of EPM

On the future prospect of EPM, a discussion should be divided into research trends and industrial applications. One of the most crucial subjects in the former is to find new functions induced by the imposition of electric and magnetic fields. A stirring of molten metals, a suppressing of liquid metal motion, a heating of metals, a levitating of metals and an eliminating of non-conductive materials in a conductive medium etc. are the well known functions based on Lorentz force. And an aligning of crystal orientation and transporting of materials are other well known functions based on Magnetization force. Recently the introduction of a high magnetic field into EPM has provided several new functions such as a generating of micro-eddy motion, so called a micro-MHD effect [28], and a patterning of non-conductive particles [29], which were found in the relation with electrodeposition reactions and based on Lorentz force. The other hand an enhancing of crystal orientation in ceramic sintering process [30, 31], enhancing of solid-solid phase transformation [32] and crystal orientation in its transformation [33] and a self-assembling and patterning of particles [34] are new functions, which have been explained from the view points of Magnetization energy or polarization effect.

Hitherto, industrial applications have been concentrated in the application of functions relating with Lorenz force and the functions of Magnetization force introduced by a high magnetic field, has